Nonpolymeric Hydrogelators Derived from Trimesic Amides

D. Krishna Kumar, D. Amilan Jose, Parthasarathi Dastidar,* and Amitava Das*

Analytical Science Discipline, Central Salt & Marine Chemicals Research Institute, G. B. Marg, Bhavnagar 364 002, Gujarat, India

Received January 21, 2004
Revised Manuscript Received April 22, 2004

Although quite a few low molecular mass organic gelators[1] (LMOGs) and their applications[2] have been reported so far, reports on supramolecular (nonpolymeric) hydrogelators are limited.[3] The occurrence of LMOG-derived hydrogelators in limited numbers is presumably due to the fact that a careful balance between hydrophobic interactions and hydrogen bonding in water is essential to achieve the required three-dimensional elastic networks involving small gelator molecules within which the water molecules are immobilized. Hydrogels display many useful properties and applications,[4] and therefore, it is of current research focus in the area of supramolecular chemistry and materials science. Herein, we report a new class of LMOG derived from pyridyl amides of trimesic acid. *N*′,*N*″,*N*‴-tris(3-pyridyl)- and *N*′,*N*″,*N*‴-tris(4-pyridyl)-trimesic amide (hereafter **1** and **2**, respectively) form hydrogel via hydrophobic interactions and hydrogen-bonding-driven self-assembly in water with the aid of organic solvents such as DMSO, MeOH, EtOH, and DMF. Multiple material properties of these compounds such as gelling ability of aqueous solvents and porous architecture with channels in the solid state as revealed by single-crystal X-ray diffraction are remarkable and probably is the first such example to the best of our knowledge.

While working in the area of organic crystal engineering[5] that led to the discovery of organic salt-based LMOGs,[6] we notice in the Cambridge Crystallographic Database[7] that mainly two types of hydrogen-bonding patterns are present in pyridine-based amides. Both the patterns are hydrogen-bonded polymeric networks, one through typical N−H...O supramolecular synthon[5a] involving the amide moiety and the other through N−H...N involving amide and pyridine ring nitrogen. Recently published single-crystal structure of **1**[8] demonstrates the occurrence of N−H...N supramolecular synthon that led to the formation of a 2-D network with hydrophobic cavity (Scheme 1a) and we reason that the corresponding 4-pyridyl derivative **2** should also self-assemble into an infinite 2-D hydrogen-bonded network involving N−H...N supramolecular synthon (Scheme 1b) as in **1**.

Scheme 1. (a) Self-assembly in 1 (as per Published Crystal Structure); (b) Expected Self-assembly in 2 through N−H...N Supramolecular Synthon

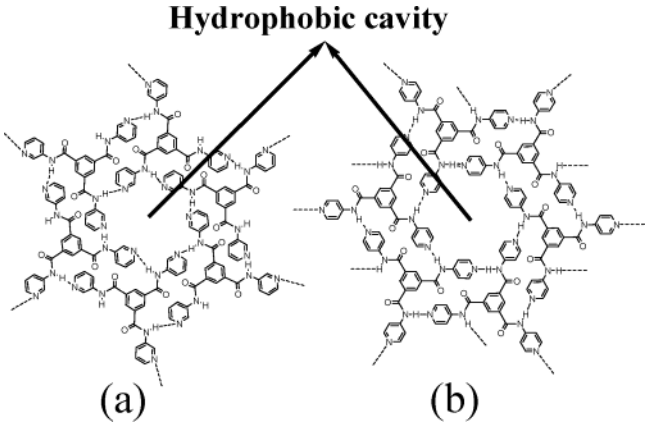

Since aggregation of gelator molecules in nonpolymeric aqueous gels are achieved through critical balance of hydrophobic effect and hydrogen bonding (if there are any), we thought that these pyridine-based trimesic amides perhaps could be good candidates for hydrogelators. Therefore, we have synthesized both **1** and **2**

* To whom correspondence should be addressed. E-mail: parthod123@rediffmail.com. Fax: +91-278-567562.

(1) (a) Terech, P.; Weiss, R. G. *Chem. Rev.* **1997**, *97*, 3133. (b) Prost, J.; Rondelez, F. *Nature* **1991**, *350*, 11. (c) Abdallah, D. J.; Weiss, R. G. *Adv. Mater.* **2000**, *12*, 1237. (d) Grownwald, O.; Shinkai, S. *Chem. Eur. J.* **2000**, *7*, 4328. (e) Jung, J. H.; Ono, Y.; Hanabusa, K.; Shinkai, S. *J. Am. Chem. Soc.* **2000**, *122*, 5008. (f) Bhattacharya, S.; Ghanashyam Acharya, S. N. *Chem. Mater.* **1999**, *11*, 3504. (g) Yamasaki, S.; Tsutsumi, H. *Bull. Chem. Soc. Jpn.* **1996**, *69*, 561. (h) Brotin, T.; Utermohlen, R.; Fages, F.; Bouas-Laurent, H.; Desvergne, J.-P. *J. Chem. Soc., Chem. Commun.* **1991**, 416. (i) Schoonbeek, F. S.; van Esch, J.; Hulst, R.; Kellog, R. M.; Ferringa, B. L. *Chem. Eur. J.* **2000**, *6*, 2633. (j) Maitra, U.; Vijay Kumar, P.; Chandra, N.; D'Souza, L. J.; Prasanna, M. D.; Raju, A. R. *Chem. Commun.* **1999**, 595. (k) Partridge, K. S.; Smith, D. K.; Kykes, G. M.; McGrail, P. T. *Chem. Commun.* **2001**, 319. (l) Bhattacharya, S.; Ghanashyam Acharya, S. N.; Raju, A. R. *Chem. Commun.* **1996**, 2101. (m) Makerević, J.; Jokić, M.; Frkaneć, L.; Kalalenić, D.; Žinic, M. *Chem. Commun.* **2002**, 2238. (n) Hanabusa, K.; Miki, T.; Taguchi, Y.; Koyama, T.; Shirai, H. *J. Chem. Soc., Chem. Commun.* **1993**, 1382. (o) Partridge, K. S.; Smith, D. K.; Kykes, G. M.; McGrail, P. T. *Chem. Commun.* **2001**, 319.

(2) (a) Kobayashi, S.; Hamasaki, N.; Suzuki, M.; Kimura, M.; Shirai H.; Hanabusa, K. *J. Am. Chem. Soc.* **2002**, *124*, 6550. (b)Jung, J. H.; Ono, Y.; Hanabusa K.; Shinkai, S. *J. Am. Chem. Soc.* **2000**, *122*, 5008. (c) Kubo, W.; Kitamura, T.; Hanabusa, K.; Wada, Y.; Yanagida, S. *Chem. Commun.* **2002**, 374. (d) Shi, C.; Huang, Z.; Kilic, S.; Xu, J.; Enick, R. M.; Beckmann, E. J.; Carr, A. J.; Melendez, R. E.; Hamilton, A. D. *Science* **1999**, *286*, 1540.

(3) (a) Estroff, L. A.; Hamilton, A. D. *Chem. Rev.* **2004**, *104*, 1201 and references therein. (b) Maitra, U.; Mukhopadhyay, S.; Sarkar, A.; Rao, P.; Indi, S. S. *Angew. Chem.. Int. Ed.* **2001**, *40*, 2281. (c) Menger, F. M.; Caran, K. L. *J. Am. Chem. Soc.* **2000**, *122*, 11679.

(4) (a) Ilmain, F.; Tanaka, T.; Kokufuta, E. *Nature* **1991**, *349*, 400. (b) Holtz, J. H.; Asher, S. A. *Nature* **1997**, *389*, 829. (c) Simonsen, L.; Hovgaard, L.; Mortensen, P. B.; Brondsted, H. *Eur. J. Pharm. Sci.* **1995**, *3*, 329. (d) Osada, Y.; Gong, J. P. *Adv. Mater.* **1998**, *10*, 827. (e) Weissman, J. M.; Sunkara, H. B.; Tse, A. S.; Asher, S. A. *Science* **1996**, *274*, 959. (f) Andrianov, A. K.; Cohen, S.; Visscher, K. B.; Payne, L. G.; Allcock, H. R.; Langer, R. *J. Controlled Release* **1993**, *27*, 69. (g) Osada, Y., Khokhlov, A. R., Eds. *Polymer Gels and Networks*; Marcel Dekker: New York, 2002. (h) Chu, Y. H.; Chen, J. K.; Whitesides, G. M. *Anal. Chem.* **1993**, *65*, 1314. (i) Lee, K.; Asher, S. A. *J. Am. Chem. Soc.* **2000**, *122*, 9534. (j) Tiller, J. C. *Angew. Chem., Int. Ed.* **2003**, *42*, 3072.

(5) (a) Desiraju, G. R. *Angew. Chem., Int. Ed. Engl.* **1995**, *34*, 2311. (b) Dastidar, P. *CrystEngComm.* **2000**, 8. (c) Ballabh, A.; Trivedi, D. R. Dastidar, P.; Suresh, E. *CrystEngComm.* **2002**, *4*, 135. (d) Trivedi, D. R.; Ballabh, A.; Dastidar, P. *CrystEngComm.* **2003**, *5*, 358.

(6) Ballabh, A.; Trivedi, D. R.; Dastidar, P. *Chem.. Mater.* **2003**, *15*, 2136. (b) Trivedi, D. R.; Ballabh, A.; Dastidar, P. C*hem.. Mater.* **2003**, *15*, 3971.

(7) Allen, F. H.; Kennard, O. *Chem. Des. Automat. News* **1993**, *8*, 3137 (CSD version 5.24, Nov. 2002).

(8) Palmans, A. R. A.; Vekemans, Jef A. J. M.; Kooijman, H.; Spek, A. L.; Meijer, E. W. *Chem. Commun.* **1997**, 2247.

10.1021/cm049881p CCC: $27.50
Published on Web 05/13/2004

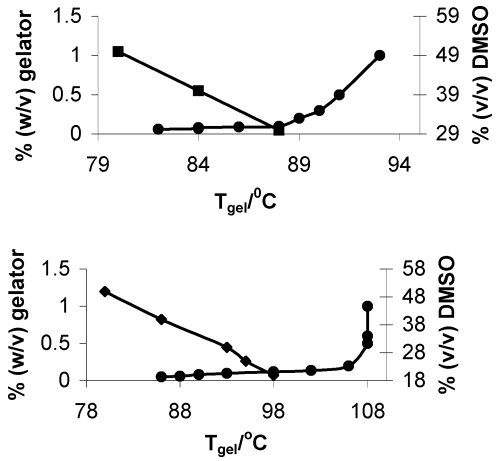

Figure 1. Plot of T_{gel} at various conditions. (●) T_{gel} vs gelator concentration; gel prepared in 3:7 DMSO/water(v/v). (◆) T_{gel} vs varying DMSO concentration in water (v/v) at a fixed concentration of 0.1 wt % gelators. Top, for **1**; bottom, for **2**.

following standard procedure.[9] To our delight, we observe that both **1** and **2** are efficient hydrogelators. Although **1** and **2** are insoluble in water, in the presence of polar solvents such as DMSO, MeOH, EtOH, and DMF, both the amides are soluble in water/organic solvent mixtures. When such mixtures are heated at ~90 °C and subsequently allowed to cool at room temperature, thermo-reversible gel (translucent) formation occurs. It is important to mention here that the thermo-reversibility experiments of MeOH/water and EtOH/water are carried out using a reflux condenser to prevent evaporation of the organic solvents from the gelling mixture. The role of the organic solvents seems to be helping the amides to be soluble in the aqueous solvent since both the amides are unable to form gels with these organic solvents alone. It may be noted here that often hydrogelators are water-insoluble and a suitable cosolvent is required to solubilize the gelator molecules in the aqueous medium.[3b,3c] DMSO/water and DMF/water gels are prepared from a 3:7 (v/v) mixture of the corresponding solvents. Both the gelators belong to the supergelator category as the minimum gel concentrations are well below 1.0 wt % (0.06 wt % for **1** and 0.04 wt % for **2** in 3:7 DMSO/water). However, MeOH/water or EtOH/water gels are prepared in a different manner. In this case, the gelator is solubilized in a minimum amount of organic solvent and a volume of water is added to it so that the final concentration of the gelator becomes 1.0 wt %. To estimate the thermal stability of the gels, the gel to sol melting temperature, T_{gel}, (Supporting Information) is plotted against the gelator concentrations (wt % w/v) in 3:7 DMSO/water (v/v) and also against varying DMSO concentrations in water (% v/v) at a fixed gelator concentration of 0.1 wt % as depicted in Figure 1.

The increase of T_{gel} with the increase of gelator concentration and also the remarkably low minimum gel concentration for both **1** and **2** indicate that self-assembly in the gel state is driven by strong intermolecular interactions. T_{gel} decreases with the increase of DMSO presumably due to the higher solubility of the gelators in excess DMSO.

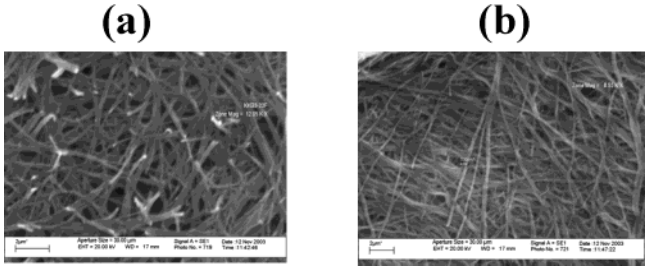

Figure 2. SEM of xerogels obtained from MeOH/water: (a) for **1** (0.2 wt %) and (b) for **2** (0.1 wt %).

FT-IR experiments are performed to gain insight into the hydrogen-bonding environment of the amide C═O group in both **1** and **2** under various conditions. In the bulk solid, an amide I band appears at 1682 and 1690 cm^{-1} with corresponding shoulders at 1658 and 1667 cm^{-1} for **1** and **2**, respectively. The shoulders are not observed upon prolonged evaporation under vacuum at 120 °C. This indicates that the C═O group in both the compounds are not homogeneously hydrogen bonded with the entrapped solvent molecules, whereas in the solution state (1661 and 1666 cm^{-1} for **1** and **2** respectively in MeOH/D_2O), significant shifts are observed (21 and 24 cm^{-1} for **1** and **2** respectively) for amide I bands. Since the positions of the amide I band in the solution state are almost the same as those observed for the corresponding shoulder peaks (in bulk solid) that disappeared upon evaporation, significant shifts may be attributed to the strong hydrogen-bonding interactions of the C═O groups with the solvent molecules in the solution state. Freshly grown crystals of **1** show the amide I band at 1681 cm^{-1}, which is virtually identical to that observed in the bulk solid. This means that, in the crystal, the C═O group is free from further hydrogen bonding with the entrapped solvent molecules, a fact that agrees well with the reported crystal structure of **1**,[8] whereas in **2**, there is a 9-cm^{-1} shift of amide I band (1681 cm^{-1}) in the crystal compared to its bulk solid. This may be attributed to weak hydrogen bonding of the C═O group with the entrapped solvent molecules in the crystal. In the gel state (MeOH/D_2O), however, the amide I band of **1** (1672 cm^{-1}) shows moderate shift of about 10 cm^{-1} compared to its bulk solid and crystal. This indicates that the C═O groups are involved in further hydrogen bonding, though weak compared to its solution state. On the other hand, the nominal 3-cm^{-1} shift of the amide I band in **2** (1678 cm^{-1}) in its gel state compared to its crystal indicates that the hydrogen-bonding environment of the C═O group of **2** is quite similar in nature both in the crystal and the gel state.

SEM pictures of the xerogel of **1** and **2** in MeOH/water ((a) and (b), respectively, in Figure 2) display a typical fibrous network of varying thickness. In the xerogel of **1**, a population of fibers (ca. 0.16−0.4 μm) could easily be seen while in that of **2**, a 3-D network of fibers (ca. 0.11−0.28 μm) is present. Understandably, the solvent molecules are immobilized in such a network of fibers resulting in gel formation.

(9) The gelator **1** and **2** were synthesized following a literature procedure (ref 8). For **2**: ^{1}H NMR (200 MHz) DMSO δ 10.94 (s, NH), 8.73 (s, 3H, H-2,4,6), 8.50 (d, 6H, H-3′,4′), 7.80 (d, 6H, H-2′,5′); IR (KBr, cm^{-1}) 3400 m, 3234 w, 3163 w, 3076 w, 2994 w, 2919 w, 2361 w, 2163 w, 1977 w, 1946 w, 1876 w, 1839 w, 1690 vs, 1667 m, 1596 s, 1512 s, 1444 m, 1416 vs, 1332 vs, 1296 s, 1281 s, 1237 s, 1211 s, 1139 m, 1099 w, 1063 w, 1000 vs, 957 w, 946 s, 919 vs, 867 s, 825 vs, 768 m, 718 vs, 675 w, 607 w, 580 s, 530 vs.

Growing single crystals of **2** for X-ray diffraction has not been straightforward due to its poor solubility in suitable solvents. Attempts to grow single crystals from MeOH and EtOH result in aqueous gel formation due to absorption of moisture. Block-shaped single crystals could finally be grown from a MeOH/DMSO (1:1) mixture in a closed vessel. The crystals, thus obtained, degrade fast due to the loss of entrapped solvents. Therefore, a suitable crystal is placed sandwiched between two layers of mother liquor in a capillary and subjected to X-ray diffraction at 100 K.[10] Unlike **1**, which crystallizes in a trigonal space group $R\bar{3}$ (No. 147),[8] the crystal of **2** belongs to monoclinic $C2/c$ (No. 15) space group and its asymmetric unit contains one molecule of the tris-amide and some disordered electron density arising from solvent molecules that could not be modeled properly. Location of one whole molecule of tris-amide in the asymmetric unit reveals that the expected C_3 symmetry of the molecule (also observed in the crystal structure of **1**) does not exist presumably due to non-symmetric rotation of $C_{aromatic}-C{=}O_{amide}$ and $N_{amide}-C_{pyridine}$ bonds, which is clear from their corresponding torsion angles.[11]

Six tris-amide molecules are self-assembled through N−H...N synthon to form an infinite 2-D sheet architecture containing hydrophobic cavities with a mean diameter of 7.812 Å (considering van der Waals radii). All the amide carbonyls, apparently not involved in hydrogen bonding, are pointing outward of the 2-D sheet and the pyridyl units are embedded inside the cavity wall. The hydrogen-bonded 2-D sheet propagates approximately parallel to the diagonal of the $a-c$ axis of the unit cell. Unlike in **1** wherein the 2-D sheets are packed almost on top of each other,[8] the corresponding packing of 2-D sheets in **2** is rather offset in nature. Even then, the channels are located down the c-axis, creating a porous structure (Figure 3).

^{1}H NMR spectra of the crystals of **2** confirm the presence of MeOH and DMSO. In TG analysis of the crystals of **2**, a two-step phase transition occurs, indicating solvent loss of 2.613% (w/w) at 232 °C and 1.989% (w/w) at 242 °C (Supporting Information). SQUEEZE[12] indicates the presence of 161 e/unit cell. This can be attributed to two molecules of DMSO (84e) and four molecules of MeOH (72e). Since six host molecules form the cavity and the unit cell contains two such cavities, 0.16 DMSO/host molecule and 0.33 MeOH/host molecule

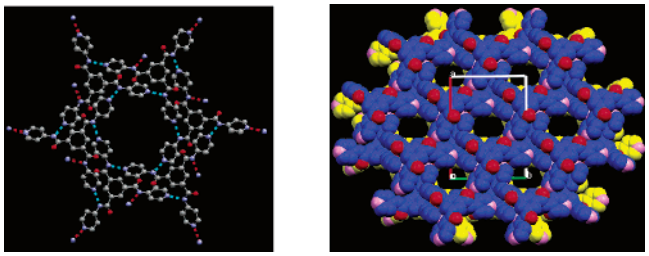

Figure 3. Left: Self-assembly of six molecules in **2** through N−H...N synthon to form hydrophobic cavity. Right: offset packing of 2-D sheets (shown in yellow and blue) in **2**, displaying the channels down the c-axis; oxygen atoms are shown in red to illustrate that they are pointing outward of the 2-D sheet.

can be assigned. 2.613% and 1.989% weight loss in TG analyses can be accredited to 0.15 DMSO and 0.28 MeOH, respectively. These values are in good agreement with the values calculated based on the SQUEEZE result. Therefore, it may be concluded that composition of host/DMSO/MeOH is 6:1:2.

To investigate the molecular packing in the gel state, attempts are made to record XRPD patterns of the gels derived from both **1** and **2**. Unfortunately, in both cases, the patterns do not show any meaningful peaks presumably due to the heavy scattering of water. The XRPD patterns of the xerogels of **1** and **2** also appear to be amorphous. This is probably due to the fact that the removal of the entrapped solvents molecules during xerogel formation causes the collapse of the crystalline superstructure, as is also observed for the corresponding single crystals.

To probe the hydrophobic pocket formation during the gelation process of **1** and **2**, a hydrophobic fluorescent probe, namely, 8-anilino-1-naphthyl sulfonic acid-Na salt (ANS−Na), is used.[13]

For this purpose, solutions of **1** and **2** in DMSO/water (3:7 v/v; [**1**] = 0.06 wt %; [**2**] = 0.05 wt %) are mixed with ANS−Na (1 μM final concentration) and the evolution of ANS−Na fluorescence with time is monitored (λ_{ex} 367 nm; λ_{em} 490 nm). Figure 4 clearly depicts that the enhancement of fluorescence intensity in both the cases follows a steady progress and after 9.0 min for **1** and 1.6 min for **2**, there is practically no enhancement, indicating gel formation. Observed enhancement is about 5-fold for **1** and 8-fold for **2** compared to the emission for ANS−Na alone in the corresponding solvent. It may be noted here that ~3-fold for **1** and ~3.3-fold for **2** in the emission intensity are observed, even in the absence of ANS−Na. This could be attributed to the scattering phenomenon arising from the poor solubility of the gelator molecules at room temperature. Similar enhancement is also observed irrespective of the excitation wavelength. Therefore, it could be concluded that the effective emission enhancement observed for **1** and **2** are 2-fold and 5-fold, respectively, considering the scattering contribution. Under identical conditions ANS−Na does not show any significant emission enhancement with time in the absence of gelator. Similarly, no detectable emission for ANS−Na is observed when it is mixed with preheated solution of **1** or **2** ([**1**] = 0.06 wt

(10) Crystal structure data for **2**: $C_{24}H_{18}N_6O_3$, formula weight = 438.44, colorless block-shaped crystals (0.29 × 0.22 × 0.18 mm), monoclinic, space group = $C2/c$ (No. 15) with a = 25.3358(19) Å, b = 15.3369(11) Å, c = 15.7647(12) Å; V = 5030.0(6) Å^3; Z = 8, D_c = 1.158 g cm^{-3}, $F(000)$ = 1824, μ(Mo Kα) = 0.080 mm^{-1}, 28309 reflections measured, 5988 unique reflections, 5420 observed reflections ($I > 2\sigma I$), R_{int} = 0.0211, 1.65° < θ < 28.26°, T = 100 K, Mo Kα radiation, graphite monochromator, λ = 0.717073 Å, on a CCD Bruker APEX diffractometer, data reduction by SAINTPLUS, structure solution and refinement by SHELXTL. Disordered solvent electron densities could not be modeled. PLATON/SQUEEZE was used to refine only the amide molecule by excluding the disordered solvent electron density which amounts to 161 e/unit cell, suggesting the presence of two molecules of DMSO and four molecules of MeOH considering TG data (see text). All nonhydrogen atoms of **2** were refined anisotropically. The amide hydrogens were located and refined. The rest of the hydrogens were fixed geometrically and refined. The final R factors R = 0.0478; wR2 = 0.1369; S = 1.027; residual electron density −0.237 and 0.352 e Å^{-3}.

(11) C(2)−C(1)-C(7)−N(9) = 38.9; C(6)−C(5)−C(25)−N(27) = 44.8; C(4)−C(3)−C(16)−N(18) = 34.9; C(25)−N(27)−C(28)−C(33) = 6.0; C(7)−N(9)−C(10)−C(11) = 17.5; C(16)−N(18)−C(19)−C(20) = 2.2°.

(12) Van der Sluis, P.; Spek, A. L. *Acta Crystallogr.* **1990**, *A46*, 194.

(13) (a) Lakowicz, J. R. *Principles of Fluorescence* Spectroscopy, Plenum: New York, 1983. (b) Preiv, A.; Zalipsky, S.; Cohen, R.; Barenholz, Y. *Langmuir* **2002**, *18*, 612.

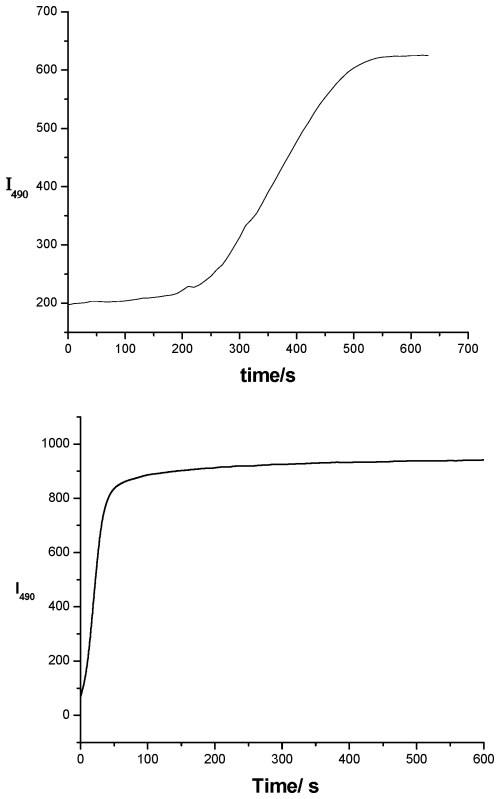

Figure 4. Time dependence of ANS−Na fluorescence during gelation of **1** (top) and **2** (bottom).

%; [**2**] = 0.05 wt %) in nongelating solvents such as DMSO. These results clearly indicate that the hydrophobic fluorophore probe must be experiencing a hydrophobic environment during the gelation process. It may be mentioned here that the presence of an hydrophobic pocket in a hydrogelator based on a steroid compound has been probed recently by similar emission experiments described herein.[3b] It is important to note that various dimensions of ANS anion calculated based on its single-crystal structure[14] suggest that at least part of the anion can certainly go into the cavity of **1** and **2** (Supporting Information).

In conclusion, we have discovered a new class of material that can be used either as hydrogelators or an inclusion host. Although the molecular packing of the gelator fibers could not be elucidated, the presence of hydrophobic pockets in the gel state is clearly established by fluorescence studies. Single-crystal structures of **1** (earlier published[8]) and **2** (present study) demonstrate porous architecture with hydrophobic cavities in these solids. It may be reasonable to assume based on single-crystal and fluorescence data that a similar self-assembly (as per crystal structure) could be responsible for hydrophobic cavity formation in the gel state.

Acknowledgment. Department of Science & Technology and Ministry of Environment & Forests, New Delhi, are thankfully acknowledged for financial support. We also thank Dr. P. K. Ghosh for his support.

Supporting Information Available: TG plot, ORTEP diagram, and hydrogen-bonding parameters for **2**, gel to sol melting temperature (T_{gel}) determination method, and chemical structure of ANS anion and its various dimensions (PDF). This material is available free of charge via the Internet at http://pubs.acs.org.

CM049881P

(14) Weber, L. D.; Tulinsky, A. *Acta Crystallogr.* **1980**, *B36*, 611.